RESEARCH ARTICLE - HYDROLOGY

Effects of anisotropic changes on the conductivity of sedimentary aquifers, southeastern Niger Delta, Nigeria

N. J George[1] · N. E Bassey[2] · A. M Ekanem[1] · J. E Thomas[1]

Abstract

Sundry soils/rocks are characterized by electrical properties with clearly or obscurely expressed anisotropies. These anisotropic effects may be low, moderate or high depending on the coefficient of anisotropy (λ). The vertical electrical sounding technique employing Schlumberger electrode configuration and lithological information from boreholes were deployed to characterize the lithological diversity in homogeneous and anisotropic geologic units that serve as aquifer systems and their overlaying layers in the coastal region of Akwa Ibom State. Based on the λ, the assessed volume of sedimentary formation is classified into low anisotropy $\lambda < 1.2$, moderate anisotropy ($1.2 < \lambda \leq 1.3$) and high anisotropy ($\lambda > 1.3$) with alluvium (64.3%), inter-bedded shale and sandstone (14.3%) and shale and slate (21.3%). The estimated percentage of respective compositional coverage indicates that alluvium is dominant, while the blended inter-bedded shale and sandstone as well as the shale and slate are minor geologic units in the Benin Formation. Inferred index of spread of alluvium indicates that the homogeneous and anisotropic units assessed are intrinsic/microscopic in nature as identified by the impressed current that passed through geologic system. The results showcased that the plot between the strike-dependent resistivity $\left(\rho_\theta\right)$ at arbitrary chosen strike and geometric mean resistivity $\left(\rho_m\right)$ can be used as a yardstick for inferring the degree of consistency of geologic compositions in homogeneous and anisotropic media. Both the quantitative (graphic) and qualitative (contour) results portend the thin possibility of having anisotropy free geologic units. The finding proposes that ground resistivity measurements and interpretations of geologic structures should be constrained by borehole information in order to firm up the intended plans for obtaining clearer, defendable and well-resolved subsurface structures.

Keywords Anisotropy · Hydrogeological units · Diversity · Strike-dependent resistivity · Sensitivity

Introduction

Most ground inhomogeneity and anisotropy induce strong directional effects on resistivity distributions and sounding curves realized from measurements (Caglar and Avsar 2007). Lithological diversity, a dynamic process, which causes electrical anisotropy of soils/rocks, is an effect of alternating beddings of arenites and argillites within the subsurface. The arenite–argillite sequence can be regarded as a medium of anisotropic diversity characterized by vertical and horizontal resistivities. Such a medium has a conductivity sensitivity, which determines the shapes of geo-electric curves. Conductivity sensitivity is the ease of soil layer/bed to conduct current that passes through them. Specifically, geo-electric curves give insights into the local geology and structure of subsurface units penetrated by the injected current (Ekanem et al. 2019; Thomas et al. 2020). As the current finds penetrates the earth, information on the primary

✉ N. J George
  nyaknnojimmyg@gmail.com; nyaknogeorge@aksu.edu.ng

  N. E Bassey
  nsikakbassey@aksu.edu.ng

  A. M Ekanem
  anny4mart@yahoo.com

  J. E Thomas
  jewelemem@gmail.com

[1] Department of Physics (Geophysics Research Group), Akwa Ibom State University, PMB 1162, Mkpat Enin, Uyo, Nigeria

[2] Department of Geology, Akwa Ibom State University, PMB 1162, Mkpat Enin, Uyo, Nigeria

geo-electrical indices, such as layer thickness (h), layer resistivity (ρ) and their corresponding depths (D) can be determined. Layer thickness is generally estimated from the depths of the layer parameters, which are initially gauged from the available VES curves. These primary geo-electric indices are estimates of importance and are used in evaluating transverse resistance ($\rho \cdot h$) and longitudinal conductance $\left(\frac{h}{\rho}\right)$ according to Hasan et al. (2019). These secondary geo-electric indices are called Dar Zarrouk parameters (DZP). Natural soils of various types have different electrical properties due to the composition, structure, water content, and temperature (George et al. 2010; Obiora et al. 2015). When the water content is below its optimum, the electrical conductivity of soils increases nonlinearly and the variation rate increases dramatically. However, when the water content is optimum, the degree of saturation, or dry density increases to a certain value and the electrical conductivity tends to be a constant. In addition, soil electrical conductivity increases with the increase in temperature, and it is observed that the electrical conductivity decreases with the increase in the number of wetting–drying cycles (Wei et al. 2013). Anisotropy is simply a condition where the earth resistivity/conductivity and hence the measured apparent resistivity/voltage is a function of the path of measurement. This anisotropy is common in clay, slate and shale, which are marked by divergent lineation or platy fabric (Greenhalgh et al. 2010). Anisotropy can exist in a macroscopic scale (Bala and Cichy 2015). Here, bands or a series of layers of divergent isotropic materials behave as they are single and equivalent anisotropic units. When anisotropy exists in a particular geologic units or minerals, it is referred to as micro-anisotropy or intrinsic anisotropy, which peculiarly depends on the crystal symmetry or texture of the material (Bala 2011). Besides the micro- and macro-anisotropies, rock cleavage, joints and fracturing, can also produce structural anisotropy peculiar to layers with alternating conductivities (rock and joint fill) Hobbs et al. (2009) and Bala and Cichy (2015). Such pseudo-anisotropy arises when the thickness of the individual isotropic bands or units is small relative to the electrode separation used for the measurement (Greenhalgh et al. 2010). The earth electrical specific resistance/resistivity deviates with the course or direction. These deviations are amply necessitated by the diversity of lithological units seen in the degree of electrical anisotropy. Permeability may be anisotropic when it changes in soils/rocks in different directions (Aissaoui et al. 2019). The effect of anisotropy exists in geologic units and if ignored, would lead to error in the interpretation of ground resistivities and the geologic structures. Some publications, which address the effects of anisotropy on surface resistivity measurements, include: Matias and Habberjam (1986), Matias (2002), Ekanem (2020). Borehole information remains the reliable means of constraining resistivity data interpretation (Asten 1974; Olasehinde and Bayewu 2011). This implies that the subsurface exhibits different electric properties in different directions (Karanth 1987; Karnkowski 1999; Yeboah-Forson and Whitman 2013). This study aims at exploring the veracity of electrical technique and geologic information in delineating the electrical conductivity sensitivity of sedimentary layers for effective understanding of the contribution of electrical resistivity in hydrogeophysical studies.

Theoretical insights

The diversity of specific resistance is based on 2 intrinsic anisotropic parameters, which are anisotropic coefficient (λ) and the average resistivity $\left(\rho_m\right)$ associated with the units of soils or rock considered (Aissaoui et al. 2019). Anisotropic diversity exists in many sedimentary formations due to permeability diversity (Bala and Cichy 2015). In homogeneously isotropic media of vertical resistivity $\left(\rho_v\right)$ and horizontal resistivity $\left(\rho_h\right)$ coefficient of anisotropy is equal to 1 as $\rho_m = \rho_h = \rho_v$ and lies between 1 and 2 for homogeneously anisotropic media characterized by anisotropy (Caglar and Avsar 2007). The coefficient of anisotropy in homogeneous and anisotropic geological unit is greater unity, because resistivity is always greatest in the transverse direction. A homogeneously isotropic unit filled with water, air or rockfield fractures is equally considered to demonstrate anisotropy. Practically, electrical current flowing perpendicularly to the soil bedding planes is largely opposed by high resistance (vertical resistivity) due a scenario that looks like series combination of resistors. Along the bedding planes, opposition to the current flow becomes comparatively reduced due to high resistance (horizontal resistivity) caused by a scenario that looks like a parallel combination of resistors. The former scenario has a higher resistivity than the later and hence explains the reason why vertical resistivity is proudly greater than the horizontal resistivity. In a formation that is homogeneous and anisotropic, with dipping angle, θ between the layer and the vertical to the direction of measurement, the electric field generates a potential difference (U) at an arbitrary point of the medium, which decreases inversely proportionally to the distance (r) from the source of the direct current, I as stated in Eq. 1

$$U = \frac{I \cdot \rho_m}{4\pi \cdot r \cdot \left(1 + \left(\lambda^2 - 1\right) \cdot \cos^2 \theta\right)^{\frac{1}{2}}} \tag{1}$$

where ρ_m is the geometric mean resistivity, the factor λ, is anisotropic coefficient defined by ρ_h and ρ_v, respectively, representing horizontal/longitudinal (minimum) resistivity and vertical/transverse (maximum) resistivity. Anisotropic coefficient (λ) is related with ρ_h and ρ_v in Eq. 2:

$$\lambda = \left(\frac{\rho_v}{\rho_h} \right)^{\frac{1}{2}} \tag{2}$$

The geometric mean resistivity $\left(\rho_m \right)$ is gauged from the horizontal and vertical resistivities as given in Eq. 3. Practically, ρ_v is the electric resistivity measured vertically to the bedding, while ρ_h is the electric resistivity measured along the bedding.

$$\rho_m = \left(\rho_v \cdot \rho_h \right)^{\frac{1}{2}} \tag{3}$$

Based on the formation values of ρ_m and λ the electric potential difference depends on the strike direction, θ along which the potential difference changes with r. In collinear array, Kunz and Moran (1958); Dachnov (1967); Greenhalgh et al. (2009), theorized that a uniform and anisotropic medium is characterized by the measured resistivity $\rho(\theta)$ which depends on the anisotropic parameters given in Eq. 4:

$$\rho(\theta) = \frac{\lambda \cdot \rho_h}{\left(1 + \left(\lambda^2 - 1\right) \cdot \cos^2 \theta\right)^{\frac{1}{2}}} = \frac{\rho_m}{\left(1 + \left(\lambda^2 - 1\right) \cdot \cos^2 \theta\right)^{\frac{1}{2}}} \tag{4}$$

The expression above shows that $\rho_m = \lambda \cdot \rho_h$. When $\theta = 0°$ and $\theta = 90°$, respectively, Eqs. 5 and 6 result from Eq. 4

$$\rho_\theta^v = \frac{\lambda \cdot \rho_h}{\lambda} = \rho_h \tag{5}$$

$$\rho_\theta^h = \lambda \cdot \rho_h \tag{6}$$

Interestingly, Eqs. 5 and 6 indicate that $\rho_\theta^v < \rho_\theta^h$ by a factor of λ. This means that the apparent resistivity $\left(\rho_\theta^v \right)$ measured normal or vertical to the strike orientation is less than apparent resistivity $\left(\rho_\theta^h \right)$ measured along the strike direction. The observed inference is in opposition to the fact that the true resistivity $\left(\rho_v \right)$ of anisotropic formation, normal to its stratification, is greater than the true resistivity $\left(\rho_h \right)$, parallel to the plane of stratification. This condition is referred to as "the paradox of anisotropy" (Aissaoui et al. 2019).

Description of location and geology of the study area

The site of the survey has an area coverage of about 435 km² within the coastal fringe of Akwa Ibom State, southeastern Nigeria. The locations of soundings fall within latitudes 4°45′–4°35′ N and longitudes 7°30′–8°10′ E in the hinterland off the Atlantic coast (Fig. 1). The area has a semi-temperate climate with distinct seasons: wet and dry seasons. The wet season commences in April and ends in September, while the dry season begins from October and ends in March. The temperature during the dry season is about 2 °C–32 °C. Annual rainfall for the area ranges between 200 and 250 cm, and can ascend to ~ 320 cm at the peak period. The area,

Fig. 1 Schematic map showing **a** the location of Akwa Ibom State, which indicate the study area and **b** the study area showing the local geology, VES points, borehole cored sample points, borehole locations and the local government boundaries
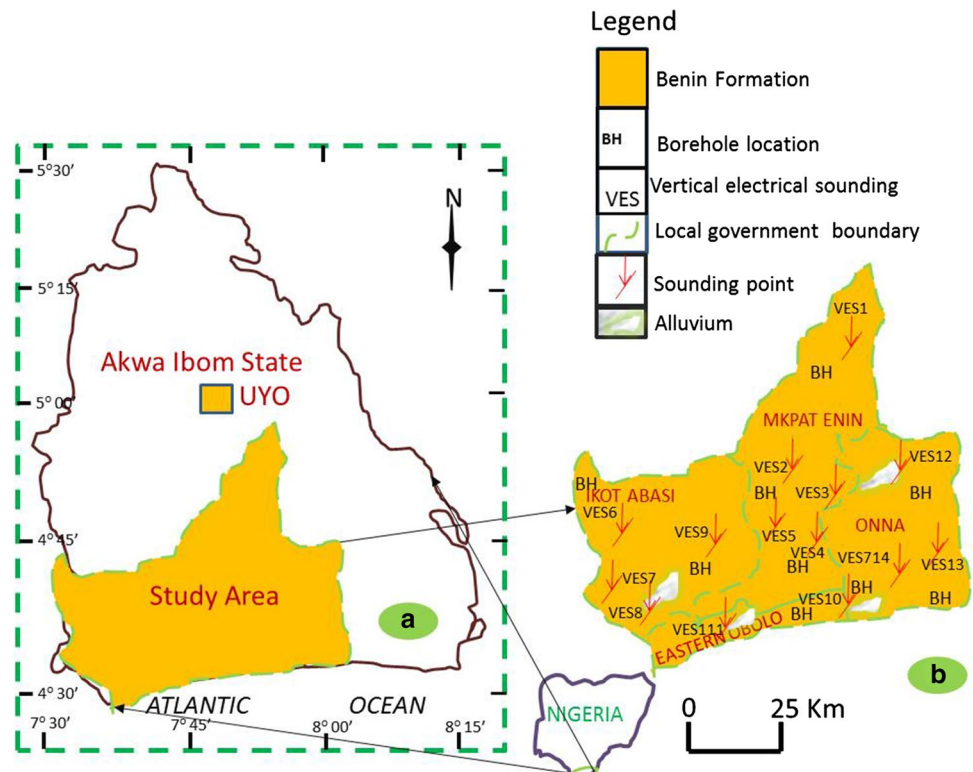
characteristically noted for its mangrove swamp is economically rich in crude oil and agricultural productions.

The area is geologically described by 3 lithostratigraphic formations. The oldest is Akata Formation (Eocene to recent) according to Peters et al. (1989), Akpan et al. (2013) and Ibanga and George (2016). This Formation exists as pro-delta facies and serves as source rock for crude oil (Short and Stauble 1967). It is opined that the shales of this formation were formed during the initial development stages of Niger Delta Basin progradation and they are compacted and over-pressured with diapiric structures such as shale swells and ridges, which intrude into the overlying younger Agbada Formation. The Agbada Formation occurs throughout Niger Delta clastic wedge as the main reservoir and seal for crude oil accumulation in the basin. It is primarily paralic deltaic front facies with maximum thickness of about 13,000 feet or 4 km (Sort and Stauble 1967). The lithologies consist of alternating system of sands, silts and shales, arranged within about 10–90 feet successions and defined by progressive upward changes in grain size and bed thickness. The depositional environment of the Agbada Formation is interpreted to be fluvial–deltaic (Short and Stauble 1967; George et al. 2015). The base of the formation extends beyond 4.5 km or 4600 feet in some areas and is defined as earliest marine shale, while the surficial parts of the formation consist entirely of non-marine sand deposited in alluvial or upper coastal plain environments during progradation of the delta (Doust and Omatsola 1989). The youngest Benin Formation in which geologic units are considered in this work is the top part of the basin clastic wedge, from the Benin–Onitsha area in the north to the coastline in the south (Short and Stauble 1967). The subsurface structure in the Niger Delta Basin spans from simple rollover faults, multiple growth faults, antithetic faults and collapsed crest faults (Onuoha and Dim 2017). These sediments formed during the Late Eocene to Early Oligocene with the reservoirs mainly controlled by pre-and syn-sedimentary tectonic elements that responded to variable rates of subsidence and sediment supply (Doust and Omatsola 1989). The hydrogeological units here are mainly brownish and believed to be developed from moderately coarse textured alluvium. Habitually, the geologic units have grayish brown, and slightly finer texture occasionally intercalated with grits.

Materials and methods

The employment of vertical electrical sounding (VES) method whose interpretation is constrained by logged borehole information as geophysical prospecting tool is a standard geophysical prospecting method. Fourteen VES data (Fig. 1) were acquired near borehole in the study area to reduce the non-uniqueness problems associated with its

interpretation and at the same time to comfortably assess the deeper subsurface sedimentary electrical resistivity information. The Schlumberger electrode configuration was used to assess vertical and longitudinal electrical conductivity distributions at shallower and deeper depths through the use of IGIS signal enhancement resistivity meter SSP-MP-ATS resistivity meter. Even though the resistivity meter has the capability to average up to 32 cycles of values, measurement cycles were truncated after 4 stacks, provided the reading on the liquid crystal display correlates well with standard deviation < 10% when direct currents were artificially injected into the earth (Yadav and Singh 2007; George 2020). Half of the current electrode separation (AB/2) ranged between 1 and 150 m and that of the potential electrode (MN/2) varied from 0.25 to 30 m. The variation in the potential electrode separation was necessary to enhance the input signal strength. When the VES field survey was completed, the VES data were modeled using the RESIST code developed by Vander Velpen and Sporry (1993) and Vander Velpen (1988). Lithological data from nearby wells were used to constrain the 1D inverse models. After a couple of iterations, a satisfactory variation between the observed field data and theoretical data were represented by means of absolute root-mean square error, which was generally found to be less than 10% (Fig. 2).

Results and discussion

Primary and secondary geo-electrical indices

The results of the VES investigation, gave a 1-D electrical resistivity, thickness and depth of geo-electrical layers given in Table 1. The current at its maximum current electrode separations penetrated 4 sedimentary layers characterized with resistivity ranges of 95.2–3455.5 Ωm and mean of 834.8 Ωm in the first layer. The second layer ranged from 8.8 to 3606.6 Ωm with mean of 1327.8 Ωm. The third and fourth layers have ranges of 72.5–1464.5 Ωm with mean 657.2 Ωm and 117.1–4893.0 Ωm with mean 1551.2 Ωm, respectively. The 4th layer was not adequately delineated as current could not penetrate this layer at the maximum current electrode separation. With the use of lithological logs from nearby boreholes, VES data were manually and electrically modeled. The statistics of each of them showed characteristic four geo-electric layers with A, HA, KQ KH and HK cluster of curves. Noticeably, due to the information from wells, resistivity values and sizable thickness of geologic units for accumulation of water in the geologic aquifers, layers 2 and 3 were identified as potential aquifers. The respective inferred thicknesses and depths vary across the sounding points with ranges 0.5–19.6 m, 1.6–56.7 m, 16.1–89.2 m and 0.5–19.6 m, 2.1–76.3 m, 20.5 m for layers 1, 3 and 3. Table 1 indicates thickness soars with
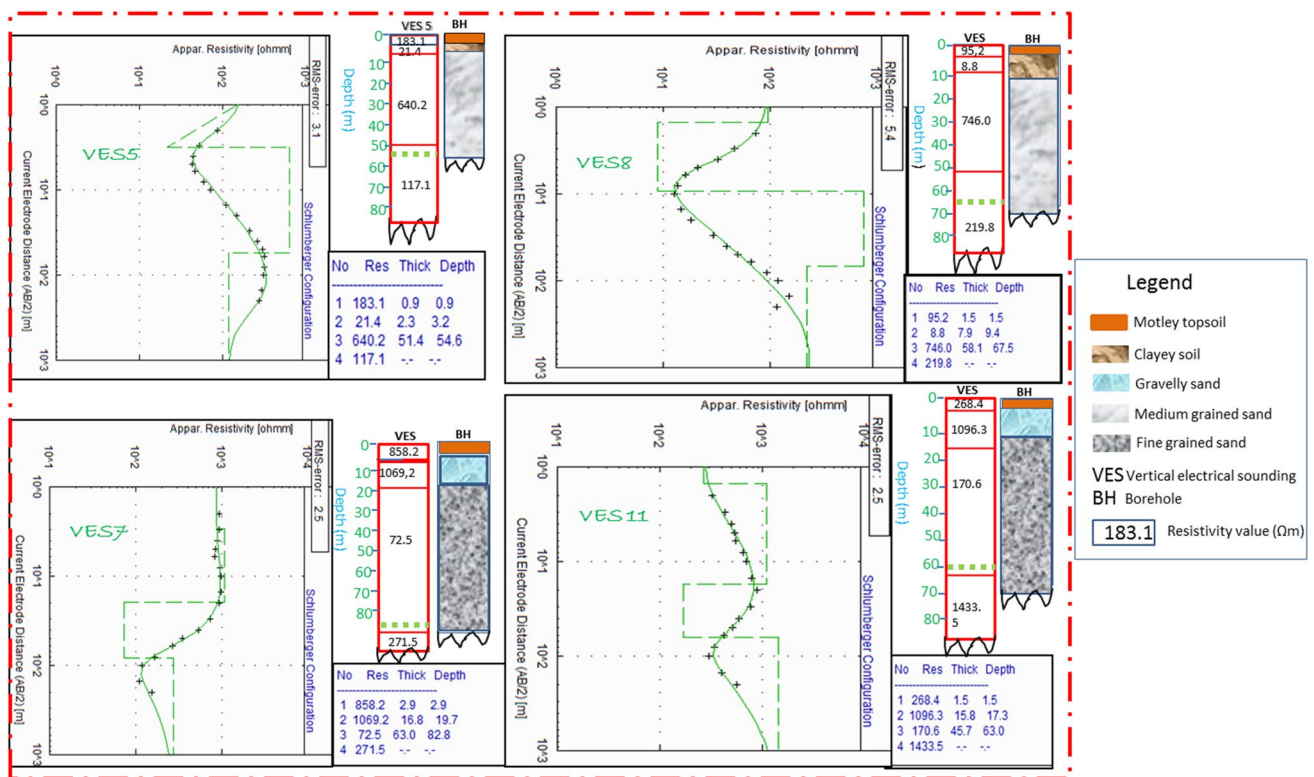
Fig. 2 Correlation of VES curves and the nearby lithology from borehole data

depth as the mean values attest. The geologic units penetrated by currents have noticeable electrical sensitivity of varying magnitudes due to intra and inter-bedded lithological diversity (Ibuot et al. 2013; George and Ekanem 2019). The hypothetical model of the subsurface in Fig. 3 identifies 2 distinct resistivities within the conducting earth units. These are the vertical (ρ_v) resistivity and the horizontal resistivity (ρ_v) estimated using Eqs. 7 and 8:

$$\rho_v = \frac{\sum_i^n h_i \rho_i}{\sum_i^n h_i} \tag{7}$$

$$\rho_h = \frac{\sum_i^n h_i}{\sum_i^n \frac{h_i}{\rho_i}} \tag{8}$$

where h_i, and ρ_i are the layer thickness and resistivity, respectively, for a given nth layer. These 2 directional parameters, defined by resistivity and thickness are directly proportional to each other. For homogeneous and anisotropic media, they are linearly related to each other by the square of average coefficient of anisotropy (Fig. 4). For the volume of homogenous and anisotropic medium that current passed through, the adjusted gradient ($\tan \theta = 0.9509; \theta \approx 44°$) for the line in

Fig. 4 is characterized by a highly correlated ($R = 0.8844$) expression given below:

$$\rho_v = 0.9508 \rho_h + 340.78 \tag{9}$$

Coefficient of anisotropy

Although the medium has adjusted average approaching unity, the geological formation is not adjudged isotropic, because the estimated values of λ ranged from values 1.00 to 2.12 with 1.22 as the mean value. Besides, the scattering in Fig. 4 shows that the formation in the layers involved is inhomogeneous and anisotropic. The disparity as noted in Fig. 5, is a valid suggested reason for departure of λ from unity. Due to homogeneous and anisotropic disparities in the assessed geological units, classification of anisotropy in the area comparatively spans from low anisotropy ($\lambda < 1.2$), moderate anisotropy ($1.2 < \lambda \leq 1.3$) and high anisotropy ($\lambda > 1.3$) with percentage of 64.3, 14.3 and 21.3%, respectively. The lower disparity between the values of ρ_v and ρ_h is tended toward lower values of λ (Fig. 5). Hence, it can be inferred that on the average, anisotropy in the area is intrinsically or microscopically induced by virtue of the consequent sequences of

Table 1 Summary of geophysics survey in the study

VES	Location	Coordinate degree		No of Layer	Layer resistivity (Ohm m)				Layer thickness (m)			Layer depth (m)			Curve type
		Lat	Long		ρ_1	ρ_2	ρ_3	ρ_4	h_1	h_2	h_3	D_1	D_2	D_3	
1	MkpatEnin	4.7752	7.7854	4	666.5	3606.6	1054.6	375.7	5.3	24.9	32.4	5.3	30.2	62.6	KQ
2	MkpatEnin	4.7345	7.7733	4	401.6	1108.4	481.9	1195.9	1.1	27.5	50.5	1.1	28.6	79.1	KH
3	MkpatEnin	4.7034	7.8758	4	395.7	1567.1	510.3	1808.6	0.6	7.9	49.3	0.6	8.5	57.8	KH
4	MkpatEnin	4.6067	7.8167	4	660.4	1488.6	549.2	1248.7	1.3	3.6	47.8	1.3	4.9	52.7	KH
5	MkpatEnin	4.6535	7.7332	4	183.1	21.4	640.2	117.1	0.9	2.3	51.4	0.9	3.2	54.6	HK
6	IkotAbasi	4.6984	7.5511	4	949.9	2715.5	1464.5	3745.2	0.5	3.9	16.1	0.5	4.4	20.5	KH
7	IkotAbasi	4.6117	7.6317	4	858.2	1069.2	72.5	271.5	2.9	16.8	63.0	2.9	19.7	82.8	KH
8	IkotAbasi	4.5767	7.5684	4	95.2	8.8	746.0	219.8	1.5	7.9	58.1	1.5	9.4	67.5	HK
9	IkotAbasi	4.6184	7.7086	4	718.4	1844.9	1362.2	1440.8	0.5	1.6	80.8	0.5	2.1	82.9	KH
10	Eastern Obolo	4.5453	7.6359	4	268.4	1096.3	170.6	1433.5	1.5	15.8	45.7	1.5	17.3	63.0	KH
11	Onna	4.7172	8.0167	4	1721.4	118.2	611.2	4893.0	19.6	56.7	36.8	91.6	76.3	113.1	HA
12	Onna	4.5689	8.0278	4	3455.5	1825.6	393.9	2030.4	0.6	2.0	89.2	0.6	2.6	91.8	HA
13	Onna	4.5997	7.8832	4	1157.0	1318.3	735.6	1585.9	1.1	37.0	47.8	1.1	38.1	85.9	KH
14	Onna	4.6629	8.0098	4	156.4	800.8	407.8	1350.1	1.3	9.1	47.9	1.3	10.4	58.3	KH
Range					95.2–3455.5	8.8–3606.6	72.5–1464.5	117.1–4893.0	0.5–19.6	1.6–56.7	16.1–89.2	0.5–91.6	2.1–76.3	20.5–113.1	
Mean					834.8	1327.8	657.2	1551.2	2.76	15.5	51.2	7.9	18.3	69.5	

Fig. 3 Hypothetical geophysical model of a homogeneous and anisotropic earth due vertically dipping beds or fractures. Transverse/vertical resistivity (ρ_v) is perpendicular to the bedding planes or fractures, while longitudinal/horizontal resistivity (ρ_h) is parallel to the bedding planes or fractures; θ, strike direction
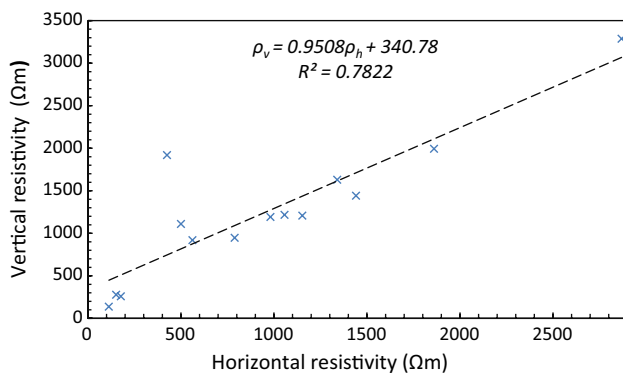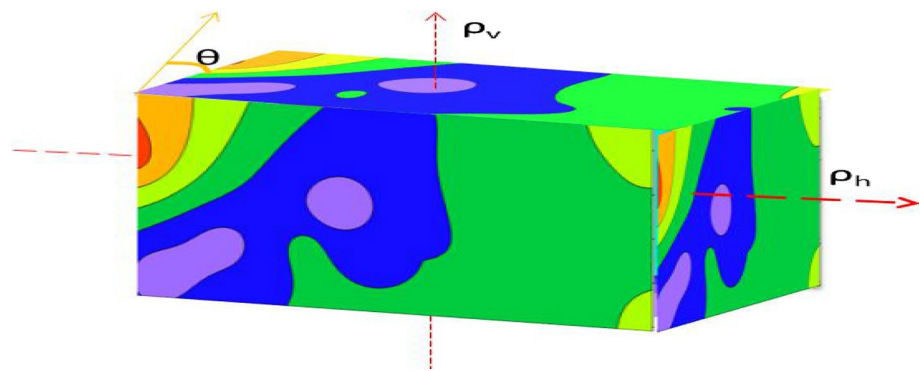
$$\rho_v = 0.9508\rho_h + 340.78$$
$$R^2 = 0.7822$$

Fig.4 A graph showing the transverse/vertical resistivity against longitudinal/horizontal resistivity

argillaceous intercalations with arenaceous sedimentary units (Greenhalgh et al. 2010). Due to sensitivity of λ to geological diversity, very narrow and typical values of λ

are associated with divergent geologic units. Based on the low coefficient of anisotropy ($\lambda < 1.2$), which covers 64.3%, the geologic units that current passed through are mainly alluvia (intercalation of clay, silt or gravel of sedimentary origin) according to the range provided by (Hill 1972; Asten 1974; Greenhalgh et al. 2010). Comparatively, moderate range of coefficient of anisotropy ($1.2 < \lambda \leq 1.3$) and elevated range ($\lambda > 1.3$), with respective 14.3 and 21.3% coverage also define the study area. These geologic units are, respectively, described as interbedded shale and sandstone as well as shale and slate by Greenhalgh et al. (2010) and are all minor formations as their percentages comparatively reflect. The absence of extremely high values of coefficient of anisotropy ($\lambda > 2.1$) indicates that there is no intrusion of metasediments into the young sedimentary age from the deeply seated basement (Greenhalgh et al. 2010). The degree of anisotropy within the unit area is well expressed in the shape of longitudinal conductance versus transverse resistance curves for layers 1–3, respectively, as revealed in Fig. 6a–c. As

Fig. 5 A diagram showing the disparity between vertical/transverse and horizontal/longitudinal resistivities within the range of coefficient of anisotropy
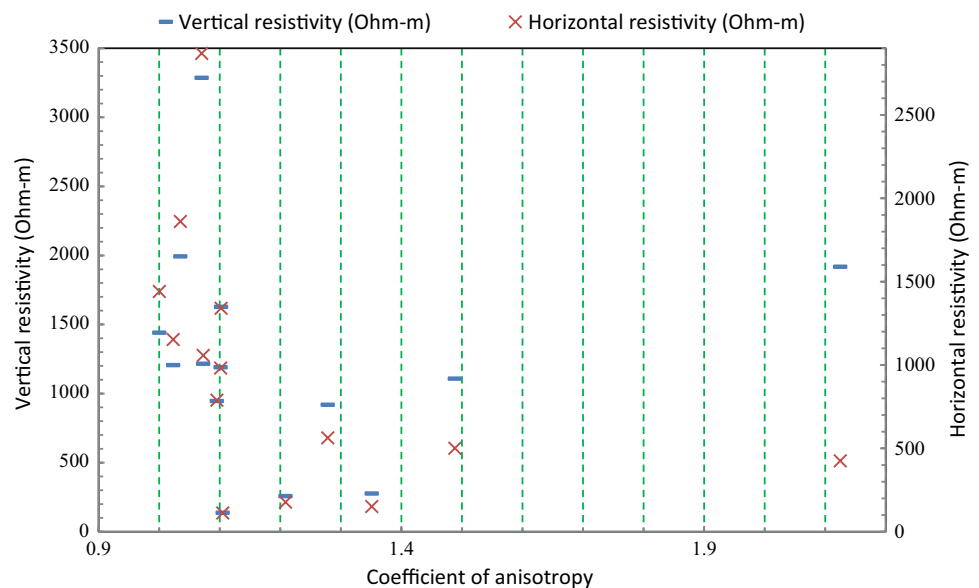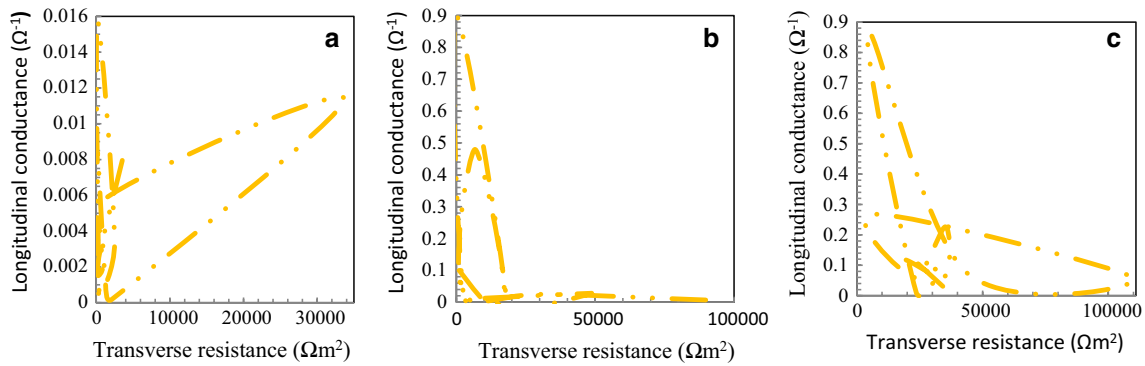
Fig. 6 Diagram showing variation of longitudinal conductivity versus transverse resistance for (**a**) layer 1, (**b**) layer 2 and (**c**) layer 3

observed in Fig. 6a–c, the values of DZP soar with depth and this showcases that thickness increases with depth. In 6a, the longitudinal conductance versus transverse resistance distribution is completely discordant with Fig. 6b and c, which are fairly consistent. The fair consistency accounts for cohesivity which is a function of depth of burial of geologic formation (George 2020).

Strike-dependent resistivity

The family of fairly collinear lines in Fig. 7 shows the relationship between resistivity, ρ_θ estimated as function of strike angle (Eq. 4) against the estimated geometric mean resistivity, ρ_m of homogeneous and anisotropic formation. The line can be summarily represented as Eq. 10:

Fig. 7 Graphs showing family of lines for strike dependence resistivity variations against mean resistivity
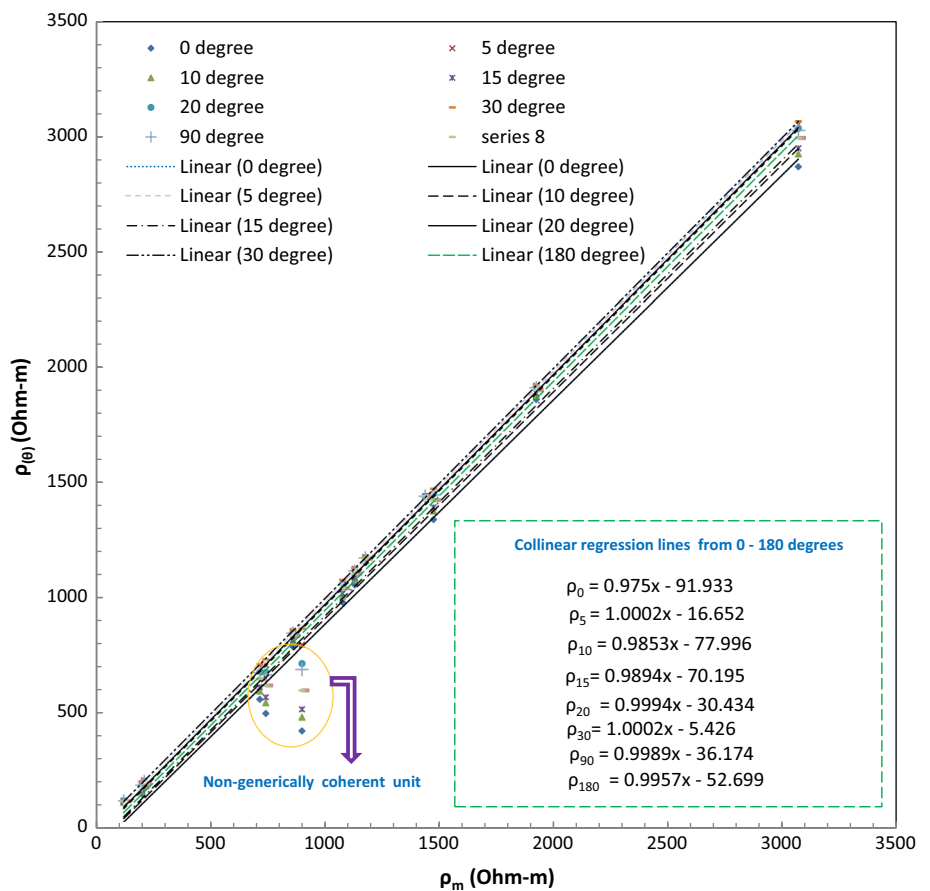
$$\rho_\theta = a\rho_m - b \qquad (10)$$

where a and b are constants representing slope and intercept. Due to consistency of intrinsic or microscopic anisotropy, the constant a appears to converge to unity as shown in the lines in Fig. 7 for strike directions θ arbitrarily chosen as 0°, 5°, 10°, 15°, 20°, 25°, 30°, 60°, 90° and 180°. The constant b becomes smaller as a converges to

unity and bigger as a marginally departs from unity. Therefore, the convergence and divergence in physical properties is function of anisotropic coefficient, which determines the strike direction. The segment of the lines with non-genetically consistent points indicate unit of non-geologically equivalent units. The contour map in Fig. 8a and b for vertical and horizontal resistivity shows consistency in the spread. This qualitative revelation is consistent with the quantitative analogy given in Fig. 4. The coefficient

Fig. 8 Diagram showing contour distributions of **a** ρ_v, **b** ρ_h and **c** λ in the stud area
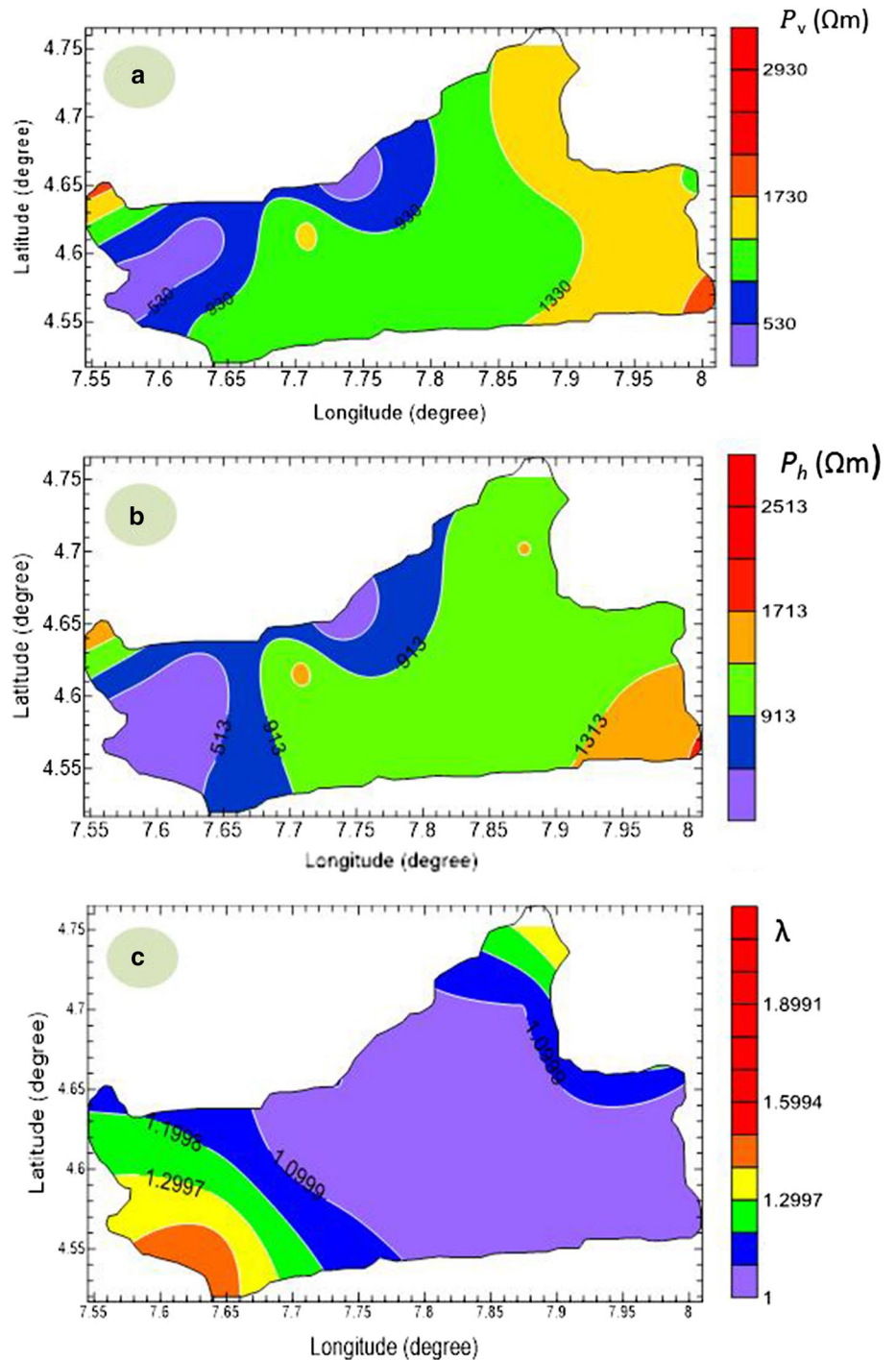
of anisotropy is Fig. 8c, shows some divergent attributes when compared to Fig. 8a and b. The displays in Fig. 8 also demonstrate that majority of the observed attributes are fairly correlated, while marginal component diverged as indicated in the color code. These graphic displays in contour map give the image of the homogeneous and anisotropic diversity, which gives room to false interpretation when in the absence of borehole information.

Conclusion

The VES technique and lithological information from boreholes were engaged to characterize the lithological diversity in homogeneous and anisotropic systems constituting the aquifer units and their overlaying layers in the hydrographic region of Akwa Ibom State. Based on the coefficient of anisotropy, the assessed volume of sedimentary formation is classified into low anisotropy ($\lambda < 1.2$), moderate anisotropy ($1.2 < \lambda \leq 1.3$) and high anisotropy ($\lambda > 1.3$) with alluvium (64.3%), inter-bedded shale and sandstone (14.3%) and shale and slate (21.3%). The respective percentage of coverage indicates that alluvium (intercalation of clay, silt or gravel of organic origin) is the dominant formation, while inter-bedded shale and sandstone as well as the shale and slate are minor geologic units. The dominant trend of alluvium indicates that the homogeneous and anisotropic units assessed are intrinsic or microscopic in nature due to the ensuing sequences of argillites intercalating with arenites in the existing hydrogeological units that the impressed current passed through. The sensitivity of current injected into the geologic units is noticeable as the delineation of fairly geologically consistent units is resolved. The absence of extremely high values ($\lambda > 2.1$) indicates that there is no intrusion of metasediments into the young sedimentary age (Greenhalgh et al. 2010). The results show that the plot between the strike-dependent resistivity versus geometric mean resistivity can be used as the basis for determining the degree of consistency of homogeneous and anisotropic geologic compositions. From this plot, it was possible to conclude the slopes of families of curves converge to unity with reduced intercepts, while slopes that marginally depart from unity are marked with high intercepts. Both the quantitative (graphic) and qualitative (contour) results portend the thin possibility of having anisotropy free geologic units. Since the effect of anisotropy really exists in geologic units either prominently or obscurely and can falsify the measured ground resistivities and geologic structure during interpretation ignored isotropic homogeneous and isotropic medium only exist in principle but not in practice. The revelations of prominent and obscured anisotropies, which coexist in hydrogeological units as revealed in Figs. 6, 7 and 8, suggest that every ground resistivity measurement and interpretation of geologic structures be accompanied or constrained by borehole information for reliability of results to be guaranteed.

Compliance with ethical standards

Conflict of interest On behalf of all authors, the there is no conflict of interest.

References

Aissaoui R, Bounif A, Zeyen H, Messaoudi S (2019) Evaluation of resistivity anisotropy parameters in the Eastern Mitidja basin, Algeria, uses azimuthal electrical resistivity tomography, Near Surface. Geophysics 17:359–378. https://doi.org/10.1002/nsg.12048

Akpan AE, Ugbaja AN, George NJ (2013) Integrated geophysical, geochemical and hydrogeological investigation of shallow groundwater resources in parts of the Ikom-Mamfe Embayment and the adjoining areas in Cross River State. Niger Environ Earth Sci 70(3):1435–1456. https://doi.org/10.1007/s12665-0132232-3

Asten MW (1974) The influence of electrical anisotropy on mise a la masse surveys. Geophys Prospect 22:238–245

Bala M (2011) Evaluation of electric parameters of anisotropic sandy-shaly miocene formations on the basis of resistivity logs. Acta Geophy 59(5):954–966

Bala M, Cichy A (2015) Evaluating electrical anisotropy parameters in miocene formations in the cierpisz deposit. Acta Geophys 63(5):1296–1315

Caglar I, and Avsar U (2007) Characterization of electrical anisotropy for cuttability of rocks using geophysical resistivity measurements, near surface in geophysics. In: 13th European meeting of environmental and engineering geophysics, Istanbul, p 3–5

Dachnov WN (1967) Electric and magnetic methods of logging. Fundament of theory, Nedra

Doust H, Omatsola E (1989) Niger Delta. In: Edwards JD, Santogrossi PA (eds) Divergent/passive margin basins, vol 48. Tulsa, American association of petroleum geologists memoir, pp 201–238

Ekanem AM (2020) Georesistivity modelling and appraisal of soil water retention capacity in Akwa Ibom State university main campus and its environs, Southern Nigeria. Model Earth Syst Environ. https://doi.org/10.1007/s40808-020-00850-6

Ekanem AM, George NJ, Thomas JE, Nathaniel EU (2019) Empirical relations between aquifer geohydraulic-geoelectric properties derived from surficial resistivity measurements in parts of Akwa Ibom State, Southern Nigeria. Nat Resour Res. https://doi.org/10.1007/s11053-019-09606-1

George NJ (2020) Appraisal of hydraulic flow units and factors of the dynamics and contamination of hydrogeological units in the littoral zones: a case study of Akwa Ibom State University and its environs, Mkpat Enin L.G.A, Nigeria. Nat Resour Res. https://doi.org/10.1007/s11053-020-09673-9

George NJ, Ekanem AM (2019) Indices of energy and appraisal for electrical current signal at polarising frequency using electrical drilling: a novel approach. In: Sundararajan N, Eshagh M, Saibi H, Meghraoui M, Al-Garni M, Giroux B (eds) On significant applications of geophysical methods: advances in science, technology and innovation (IEREK Interdisciplinary Series for Sustainable Development). Springer, Cham. https://doi.org/10.1007/978-3-030-01656-2_21

George JG, Ekanem AM, Ibanga JI, Udosen NI (2017) Hydrodynamic implications of aquifer quality index (AQI) and flow zone indicator (FZI) in groundwater abstraction: a case study of coastal hydro-lithofacies in South-eastern Nigeria. J Coast Conserv 21(4):759–776. https://doi.org/10.1007/s11852-017-0535-3

George NJ, Ibanga JI, Ubom AI (2015) Geoelectrohydrogeological indices of evidence of ingress of saline water into freshwater in parts of coastal aquifers of IkotAbasi. South Niger J Afri Earth Sci 109:37–46

George NJ, Obianwu VI, Akpan AE, Obot IB (2010) Assessment of shallow aquiferous units and their coefficients of anisotropy in the coastal plain sands of Southern Ukanafun local government area, Akwa Ibom State. South Niger Arch Phys Res 2:118–128

Greenhalgh SA, Marescot L, Zhou B, Greenhalgh M, Wiese T (2009) Electric potential and Frechet derivatives for a uniform anisotropic medium with a tilted axis of symmetry. Pure Appl Geophys 166:673–699

Greenhalgh S, Wiese T, Marescot L (2010) Comparison of DC sensitivity patterns for anisotropic and isotropic media. J Appl Geophys 70(2010):103–112. https://doi.org/10.1016/j.jappgeo.2009.10.003

Hasan M, Yanjun S, Gulraiz A, Weijun J (2019) Application of VES and ERT for fresh-saline interface in alluvial aquifers of Lower Bari Doab, Pakistan. J Appl Geophys 164:200–213

Hill DG (1972) A laboratory investigation of electrical anisotropy in Precambrian rocks. Geophysics 37:1022–1038

Hobbs B, Werthmuller D, Engelmark F (2009) The effect of resistivity anisotropy on earth impulse responses. ASEG Ext Abstr 2009:1–5

Ibanga JI, George NJ (2016) Estimating geohydraulic parameters, protective strength, and corrosivity of hydrogeological units: a case study of ALSCON, Ikot Abasi, southern Nigeria. Arab J Geosci 9:363. https://doi.org/10.1007/s12517-016-2390-1

Ibuot JC, Akpabio GT, George NJ (2013) A survey of the repository of groundwater potential and distribution using geo-electrical resistivity method in Itu Local Government Area (L.G.A), Akwa Ibom State, Southern Nigeria. Cent Eur J Geosci 5(4):538–547. https://doi.org/10.2478/s13533-012-0152-5

Karanth KR (1987) Groundwater assessment, development and management. Tata-McGraw Hill, New Delhi

Karnkowski P (1999) Oil and gas deposits in Poland. Geosynoptics Society (GEOS), Krakow

Kunz KS, Moran JH (1958) Some effects of formation anisotropy on resistivity measurements in boreholes. Geophysics 23(4):770–794. https://doi.org/10.1190/1.1438527

Matias MJS (2002) Square array anisotropy measurements and resistivity sounding interpretation. J Appl Geophys 49:185–194

Matias MJS, Habberjam GM (1986) The effect of structure and anisotropy on resistivity measurements. Geophysics 51:964–971

Obiora DN, Ibuot JC, George NJ (2015) Evaluation of aquifer potential, geoelectric and hydraulic parameters in Ezza North, southeastern Nigeria, using geoelectric sounding. J Sci Technol Int. https://doi.org/10.1007/s13762-015-0886-y

Olasehinde PI, Bayewu OO (2011) Evaluation of electrical resistivity anisotropy in geological mapping: a case study of Odoara, West Central Nigeria. Afr J Environ Sci Technol 5(7):553–566

Onuoha KM, Dim CIP (2017) Developing unconventional petroleum resources in Nigeria: an assessment of shale gas and shale oil prospects and challenges in the inland Anambra Basin. In: Onuoha KM (ed) Advances in petroleum geoscience research in Nigeria, Chapter 16, 1st edn. University of Nigeria, Nsukka, pp 313–328

Petters SW (1989) Akwa Ibom State: physical background, soil and landuse and ecological problems. In: Technical report for government of Akwa Ibom State, pp 603

Short KC, Stauble AJ (1967) Outline of the geology of Niger Delta. Assoc Pet Geol Bull 54:761–779

Thomas JE, George NJ, Ekanem AM, Nsikak EE (2020) Electrostratigraphy and hydrogeochemistry of hyporheic zone and water-bearing caches in the littoral shorefront of Akwa Ibom State University, Southern Nigeria. Environ Monit Assess 192:505. https://doi.org/10.1007/s10661-020-08436-6

Vander-Velpen BPA (1988) A computer processing package for D.C. resistivity interpretation for an IBM compatibles. ITC, The Netherlands, p 4

Vander Velpen BPA, Sporry RJ (1993) RESIST: a computer program to process resistivity sounding data on PC compatibles. Comput Geosci 19(5):691–703

Wei B, Lingwei K, Aiguo G (2013) Effects of physical properties on electrical conductivity of compacted lateritic soil. J Rock Mech Geotech Eng 5(5):406–411

Yadav GS, Singh SK (2007) Integrated resistivity surveys for delineation of fractures for ground water exploration in hard rock areas. J Appl Geophys 62(3):301–312

Yeboah-Forson A, Whitman D (2013) Electrical resistivity characterization of anisotropy in the Biscayne Aquifer. Groundwater 52(5):728–736